Entanglement Rules for Random Mixtures

J. Duplat,[1] A. Jouary,[1] and E. Villermaux[2,*]
[1]Aix-Marseille Université, IUSTI, 13453 Marseille Cedex 13, France
[2]Aix-Marseille Université, IRPHE, 13384 Marseille Cedex 13, France
(Received 14 April 2010; published 16 July 2010)

We discuss how two subparts of a randomly stirred scalar mixture interact to form the overall concentration distribution. We derive, in particular, the appropriate composition laws in the absence and presence of a strong correlation between the fields. The resulting concentration distributions compare favorably with several distinct experiments, illustrating the two limits. The initial relative spatial position of the subparts plays a crucial role on the nature of their subsequent entanglement.

DOI: 10.1103/PhysRevLett.105.034504 PACS numbers: 47.51.+a, 47.27.wj

Understanding how correlations arise in a complex system, and how they determine the future of the system itself is a pivotal aspect of the physics of irreversible processes. Scalar mixing is a paradigm of such systems: stirring a blob of dye in a clear substrate leads irreversibly to a uniform medium with average concentration. The interesting question is to understand the route toward uniformity and the transient stages when the scalar concentration C is distributed according to a certain probability distribution $P(C)$, depending on time. At least in some circumstances, the interaction between the fluid particles with different concentrations is crucial for the fate of the mixture. Curl [1] has first proposed the simplest idealized vision: particles meet at random, coalesce in equalizing their concentration before breaking up to meet other particles, in a sequential fashion. This kind of construction, assuming no correlation between the elements merging at random, has been since then generalized and used in several different contexts [2–6]. However, recent work on scalar mixing has emphasized the role of correlations in real space on the statistical content of random mixtures [7,8]. Here, we conduct a discussion at the level of the concentration distribution itself, wondering how the presence, or absence of correlation in the medium determine the construction law of $P(C)$.

We consider the simultaneous mixing of two inks (red and green) with identical molecular diffusivities in a transparent diluting medium, under a given stirring protocol. The situation can be viewed as the interaction of two sources [9–11], obviously relevant when the species are reactive [12,13]. Alternatively, the fields C_R and C_G can be interpreted as two subparts of one single total concentration field

$$C = C_R + C_G \tag{1}$$

as if, in Fig. 1 for instance, one confuses red and green fields into a single white spot diluting into a dark environment [5]. These two subparts of the concentration field, each singled out by their own color, will each give rise, as stirring proceeds, to a given concentration distribution $P_R(C_R)$ and $P_G(C_G)$. From the interaction of these two fields will result the distribution of the total field $P(C)$. Deciphering the nature of this interaction, namely, finding the relation between $P(C)$ and the source fields $P_R(C_R)$ and $P_G(C_G)$, is the subject of this Letter.

The signature of the interaction between the fields is all encoded in the joint probability $Q(C_R, C_G)$ of finding both concentrations C_R and C_G at the same location in the medium. An ersatz of the information contained in $Q(C_R, C_G)$ is the correlation coefficient

$$\chi = \frac{\langle (C_R - \langle C_R \rangle)(C_G - \langle C_G \rangle) \rangle}{\sqrt{\sigma_R^2 \sigma_G^2}}, \tag{2}$$

where $\langle \cdot \rangle$ is the average over $Q(C_R, C_G)$, and $\sigma_\alpha^2 = \langle (C_\alpha - \langle C_\alpha \rangle)^2 \rangle$ is the variance of the individual fields $\alpha = R, G$. With a sign depending if the concentrations fields are in phase, or in phase opposition, χ lies in the range $[-1, 1]$. For independent fields, χ is zero (a property whose reciprocal is wrong). In the same way the total concentration distribution $P(C)$ can be computed from the joint probability $Q(C_R, C_G)$, the correlation coefficient χ derives from

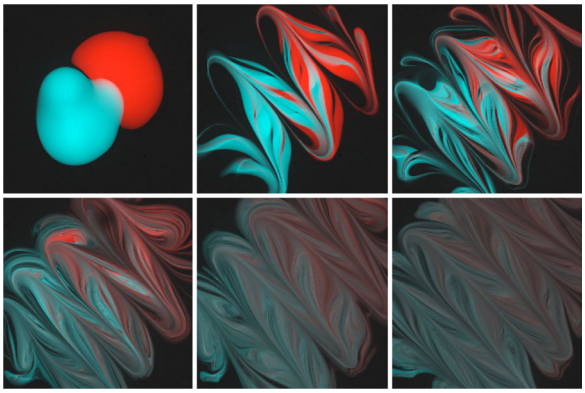

FIG. 1 (color online). Mixing of two ink spots in a viscous medium, initially laid side by side. The concentration field resulting from the stirring protocol defined in [5] is shown after 1, 2, 5, 8, and 11 cycles.

$P(C)$ as

$$\chi = \frac{\sigma^2 - \sigma_R^2 - \sigma_G^2}{2\sqrt{\sigma_R^2 \sigma_G^2}} \tag{3}$$

and thus appears as a global index measuring the interactions between the fields. Let us now make precise what interaction means, and explore possible scenarios for the construction of $P(C)$:

(1) For C_R and C_G being independent fields, one has $Q(C_R, C_G) = P_R(C_R)P_G(C_G)$ and

$$P(C) = \int_{C=C_R+C_G} P_R(C_R)P_G(C_G)dC_R \tag{4}$$

is the convolution of $P_R(C_R)$ and $P_G(C_G)$, as suitable for independent variables [14]. This defines the interaction rule with a correlation coefficient χ equal to zero.

(2) For C_R and C_G strongly correlated, ordering the field by increasing values of C_R is equivalent with ordering the field by increasing values of C_G. Calling $\mathcal{F}_\alpha$ the cumulative distribution of P_α

$$\mathcal{F}_\alpha(C_\alpha) = \int_0^{C_\alpha} P_\alpha(C)dC, \tag{5}$$

if $\mathcal{F}_R(C_R)$ and $\mathcal{F}_G(C_G)$ are equal (say to x), then the concentrations C_R and C_G lay on the same spatial subset. Consequently,

$$\forall\ x \in [01], \qquad \mathcal{F}^{-1}(x) = \mathcal{F}_R^{-1}(x) + \mathcal{F}_G^{-1}(x), \tag{6}$$

where $\mathcal{F}^{-1}(x)$ is the reciprocal function of $\mathcal{F}(C)$. $\mathcal{F}$ and P are thus computed implicitly, defining the maximal correlation coefficient $\chi_{\max}$ through Eq. (3). With $\partial_x[\mathcal{F}^{-1}(x)] = 1/\partial_C[\mathcal{F}(C)]$, one also has $1/P(C) = 1/P_R(C_R) + 1/P_G(C_G)$, holding whenever an increasing morphism between C_R and C_G exists. In particular, when the morphism is linear (i.e., P_R and P_G are similar), $\chi_{\max} = 1$. The limit where the fields are negatively correlated ($\chi < 0$) can be treated along the same lines.

We now investigate how the two scenarios we have described help in understanding several experiments.

A first experiment consists in stirring two nearby colored ink spots in a glycerin layer by a rod. The two spots are initially side by side, with no overlap. A number of parallel cuts with amplitude L is made in one direction and then the same number in the orthogonal direction, defining a stirring cycle. Cycles are repeated iteratively, and so proceeds the mixture toward uniformity (see Figs. 1 and 5 for protocol details). At each cycle, the concentration field is imaged with a color digital camera, allowing the red and green fields to be extracted independently. Concentrations C_R and C_G are made nondimensional by their initial value. After a few mixing cycles, the ink spots have dispersed and are intermingled in a large subset of the glycerin layer. The individual probability distribution $P_R(C_R)$ and $P_G(C_G)$ are composed of a Dirac delta at $C = 0$ corresponding to the external diluting medium, plus a bell shaped distribution close to a Gamma distribution [5]. As seen in Fig. 2, the total distribution $P(C)$ presents higher concentration levels than those in the individual fields. The part of the distribution with nonzero concentrations corresponds to the entanglement of the initial spots. Even at the earliest stages of the stirring protocol, the independence scenario in Eq. (4) succeeds very well in constructing $P(C)$ from the convolution of $P_R(C_R)$ and $P_G(C_G)$. Note, however, that only the bell shaped parts of the individual distributions have been convoluted to compare with the measured $P(C)$ (i.e., the Dirac delta is excluded): a strong correlation obviously exists between the diluting support of the red and green fields. However, inside the entangled support of the dyed fields, C_R and C_G are independent.

A second experiment is performed by discharging two fluorescent dyes (red rhodamine and green disodium fluorecein) through two adjacent tubes in a diluting water stream at the inlet of a square transparent duct. The velocity of the diluting coflow is set equal to the injection velocities in the tubes, and the average concentrations $\langle C_R \rangle$ and $\langle C_G \rangle$ are conserved along the duct in this confined geometry. The flow is turbulent and the concentration fields are made visual by a plane argon laser sheet slicing the duct along its axis (see [5] for details).

Near the injection point, the two plumes are segregated ($\chi = -1$). Farther downstream (beyond three cross section widths L typically), the two plumes are intermingled into an entangled set of sheets, as seen in Fig. 3. The total concentration distribution $P(C)$ results accurately from the convolution of the individual fields $P_R(C_R)$ and

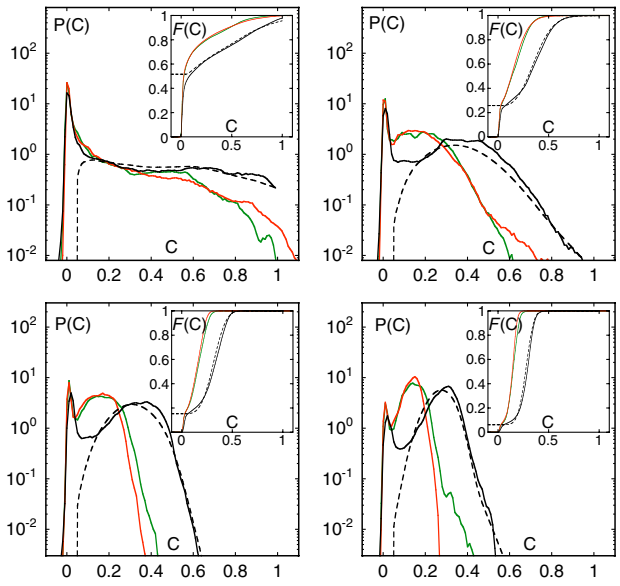

FIG. 2 (color online). Concentration distributions $P(C)$ for the red and green dyes in Fig. 1, and for the total concentration field (black line), at cycles 2, 5, 8, and 11. The total distribution is compared with the convolution rule in Eq. (4) (dotted line). The insets show the corresponding cumulative distributions $\mathcal{F}(C)$.

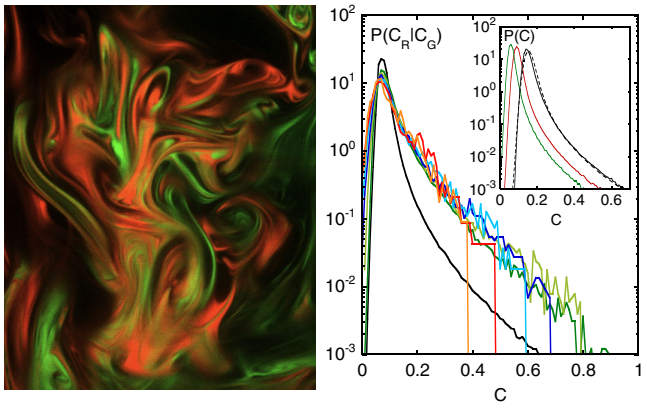

FIG. 3 (color online). Left: Mixing pattern of two dyes in a turbulent channel flow at a downstream distance $5L$ with L the channel width. Right: Conditional distribution $P(C_R|C_G)$ of the red concentration, for fixed green concentration $C_G = \{0, 0.1, 0.2, 0.3, 0.4, 0.5, 0.6\}$ at distance $5L$. Insert: Distribution of red, green, and total concentration (respectively in red, green, and black) and comparison with Eq. (4) (dashed line).

$P_G(C_G)$, indicating that C_R and C_G are, in that case also, independent variables in the flow. The inspection of the conditional distribution $P(C_R|C_G)$ such that $P_G(C_G)P(C_R|C_G) = Q(C_R, C_G)$ makes this statement more accurate: $P(C_R|C_G)$ is independent of C_G for any $C_G > 0.1$, and for C_R comprised between 0 and $1 - C_G$. In other words, a fluid particle from the, say, red field has statistically in its immediate environment all the concentration levels contained in the green field at that location. Because the total concentration C cannot exceed 1, $P(C_R|C_G)$ vanishes for C_R larger than $1 - C_G$. Also apparent in Fig. 3 is that for C_G close to 0, the probability that C_R is also small is in excess (black curve). This indicates the presence of void regions in the flow, no invaded by any of the two initially dyed streams, and which are the analogue of the diluting region whose signature is the Dirac delta in the distributions of Fig. 2.

Both in a viscous two-dimensional, and a turbulent three-dimensional flow, initially segregated scalar sources (with $\chi = -1$) finally entangle and superimpose in an independent manner ($\chi = 0$) under the action of stirring. These observations are consistent with known facts concerning the interaction of thermal plumes from heated wires in high Reynolds number wind tunnel turbulence [9,10,15]. In this configuration, the time required for two plumes to entangle depends on their initial separation, and once they have a common support, the individual concentration fields (restricted to the common support) are independent. The observed reincrease of χ to positive values is due to the positive correlation with the void regions on both sides of the merged plume (called external intermittency in this context), playing the same role as the diluting medium in the experiments above.

When the sources give rise to independent concentrations fields, the total concentration distribution is the convolution of the individual distributions [Eq. (4)]. Since the color coding of the subparts of the initial scalar field has been made arbitrarily, one might expect that the total concentration distribution $P(C)$ itself will evolve in a self convolution way. That remark, whose relevance is demonstrated here, has been conjectured earlier and led to a prediction for the functional form of $P(C)$, found to be a family of Gamma distributions representing well, in some cases, actual random mixtures (see [5,16] for a more elaborated presentation). However, minute modifications of the initial scalar spatial pattern of the sources make the

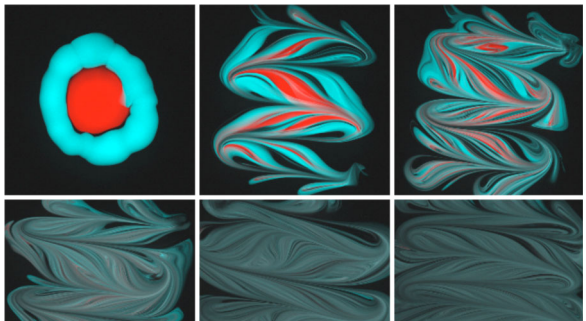

FIG. 4 (color online). Mixing of two ink spots in a viscous medium, initially deposited concentrically. The concentration field resulting from the stirring protocol defined in [5] is shown after 1, 2, 5, 8, and 10 cycles.

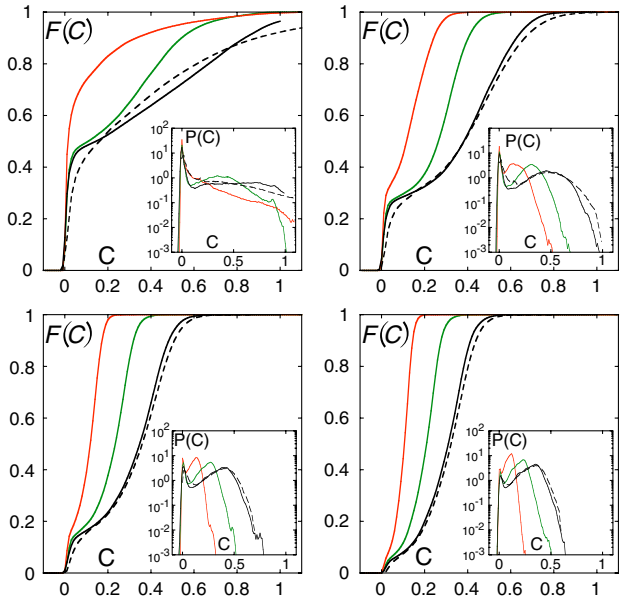

FIG. 5 (color online). Cumulative distribution $\mathcal{F}(C)$ for the red and green dyes in Fig. 4, and for the total concentration field at cycle 2, 5, 8, and 10. The total distribution is compared with the correlated rule in Eq. (6). The insets show the corresponding distributions $P(C)$.

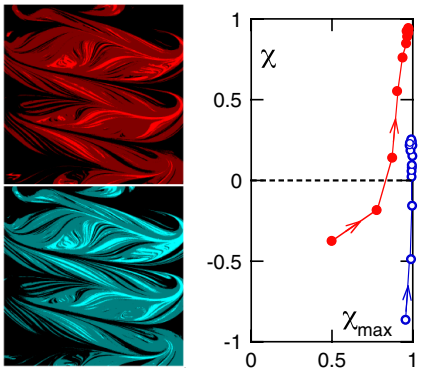

FIG. 6 (color online). Left: Spatial sets at cycle 8 in Fig. 4 for $\mathcal{F}_R(C_R) = \mathcal{F}_G(C_G) = x$ with $x = 0.5$ (shaded) and $x = 0.95$ (bright) for red and green fields, demonstrating their strong spatial correlation ($\chi \approx 0.9$). Right: Correlation coefficient χ versus its maximal reachable value $\chi_{\max}$ in Eq. (6) for Fig. 1 (empty labels), and Fig. 4 (filled labels), as cycles proceed (arrow).

nature of the subsequent interaction between the fields drastically different.

Consider a slightly modified version of our first experiment of stirring in a viscous two-dimensional layer (Fig. 1). Only the initial condition differs: now the two spots are deposited concentrically in the medium (Fig. 4). In that case, the convolution rule in Eq. (4) fails at reconstructing the total field $P(C)$, now given by the strong correlation rule in Eq. (6), as seen in Fig. 5. The final correlation coefficient χ is about 0.9 (Fig. 6).

In the experiment of Fig. 1, the initial separation of the blobs is of the order of the stirring rod amplitude motion L. A lamellae formed from one of the spots has thus an individual stretching history independent from the one of the lamellae of the other spot with which it will ultimately merge in the entangled set, hence the success of the independency rule. On the contrary, the two fields are sliced together from the start with the initial condition of Fig. 4, and therefore stick to each other along their whole history in the medium, hence their correlation, obvious in Fig. 6 showing that the spatial locations for a given threshold x in Eq. (6) are identical for both the C_R and C_G fields in this experiment.

Instead of two, one can consider that our experiments involve three colors: red, green (R, G), and a background color (B). By mass conservation, $C_R + C_G + C_B = 1$ at all times. Writing concentrations as a sum of an average plus fluctuations as $C_\alpha = \langle C_\alpha \rangle + c_\alpha$, one has $c_B = -(c_R + c_G)$. Consequently, the correlation of red and green fields writes $\langle c_R c_G \rangle = \frac{1}{2}(\langle c_B^2 \rangle - \langle c_R^2 \rangle - \langle c_G^2 \rangle)$. Hence the sign of the correlation coefficient can be positive only if $\langle c_B^2 \rangle$ is large enough in the intermingled set. The role of the external fluid is besides crucial: as mentioned, we subtract the outer background from the fields (the Delta peak at $C_{R,G} = 0$) when composing them.

Iterated random motions on a scalar field form stretched lamellae in two dimensions, and sheets in three dimensions. The concentration field is constructed from the diffusive merging of these elementary sheets in bundles whose width defines the correlation distance of the concentrations. This coarsening scale is proportional to the stirring scale L times a correction function of the scalar diffusivity [17]. Initially distant subparts of the scalar field are likely to have independent histories in the medium before merging and defining $P(C)$, while nearby regions are, and remain correlated.

*Also at Institut Universitaire de France, Paris, France.
villermaux@irphe.univ-mrs.fr

[1] R. L. Curl, AIChE J. **9**, 175 (1963).
[2] S. B. Pope, Prog. Energy Combust. Sci. **11**, 119 (1985).
[3] A. Pumir, B. I. Shraiman, and E. D. Siggia, Phys. Rev. Lett. **66**, 2984 (1991).
[4] C. Dopazo, in *Turbulent Reacting Flows*, edited by P. A. Libby and F. A. Williams (Academic Press, London, 1994), Chap. 7.
[5] E. Villermaux and J. Duplat, Phys. Rev. Lett. **91**, 184501 (2003).
[6] R. O. Fox, *Computational Models for Turbulent Reacting Flows* (Cambridge University Press, Cambridge, 2004).
[7] B. I. Shraiman and E. D. Siggia, Nature (London) **405**, 639 (2000).
[8] G. Falkovich, K. Gawedzki, and M. Vergassola, Rev. Mod. Phys. **73**, 913 (2001).
[9] Z. Warhaft, J. Fluid Mech. **144**, 363 (1984).
[10] E. Costa-Patry and L. Mydlarski, J. Fluid Mech. **609**, 349 (2008).
[11] S. Viswanathan and S. B. Pope, Phys. Fluids **20**, 101514 (2008).
[12] S. Komori, J. Hunt, T. Kanzaki, and Y. Murakami, J. Fluid Mech. **228**, 629 (1991).
[13] R. J. Brown and R. W. Bilger, Atmos. Environ. **32**, 629 (1998).
[14] W. Feller, *An Introduction to Probability Theory and Its Applications* (John Wiley & Sons, New York, 1970).
[15] Z. Warhaft, J. Fluid Mech. **104**, 93 (1981).
[16] J. Duplat and E. Villermaux, J. Fluid Mech. **617**, 51 (2008).
[17] E. Villermaux and J. Duplat, Phys. Rev. Lett. **97**, 144506 (2006).